ELSEVIER

Synthetic Metals 118 (2001) 1–9

SYNTHETIC METALS

www.elsevier.com/locate/synmet

The interplay of efficiency and morphology in photovoltaic devices based on interpenetrating networks of conjugated polymers with fullerenes

D. Gebeyehu[a], C.J. Brabec[a,*], F. Padinger[b], T. Fromherz[b], J.C. Hummelen[c], D. Badt[d], H. Schindler[d], N.S. Sariciftci[a]

[a]*Christian Doppler Laboratory for Plastic Solar Cells, Institute of Physical Chemistry, Johannes Kepler University of Linz, Altenbergerstr. 69, A-4040 Linz, Austria*
[b]*Quantum Solar Energy Linz, A-4040 Linz, Austria*
[c]*Stratingh Institute & Materials Science Center, University of Groningen, Nijenborgh 4, 9747 AG Groningen, The Netherlands*
[d]*Institute for Biophysics, Johannes Kepler University of Linz, Linz, Austria*

Received 9 February 2000; received in revised form 3 April 2000; accepted 3 April 2000

Abstract

Photophysical phenomena in composites of fullerenes and non-degenerate ground state conjugated polymers with highly extended π-electrons in their main chain can be explained by the ultrafast electron transfer from the conjugated polymer (donor) to the fullerene (acceptor) upon illumination. In this work we present current/voltage characteristics, efficiency data and surface morphology studies of large area (6 cm×6 cm) flexible plastic solar cells with a photoactive layer consisting of poly(2-methoxy-5-(3′,7′-dimethyloctyloxy)-1,4-phenylene vinylene), (MDMO-PPV) or poly(3-octylthiophene), (P3OT) as donor and fullerene C_{60} or a highly soluble methanofullerene, (phenyl-[6,6]-C_{61})-butyric acid methyl ester (PCBM) as electron acceptor. Solar cell devices have been fabricated showing monochromatic energy conversion efficiencies η_e about 1.5% and carrier collection efficiency (incident photon-to-collected electron, IPCE) of 20% at 488 nm under 10 mW/cm^2. Furthermore, we have investigated the quality and homogeneity of the photoactive composite films made from the various components. It is shown that among the combinations of materials both open circuit voltage and short circuit current are maximal for blends of P3OT/C_{60} and MDMO-PPV/PCBM.

Keywords: Solar cells; Poly(*para*-phenylenevinylene) (PPV) and derivatives; Polythiophene and derivatives; Fullerene; Methanofullerene; Metal/semiconductor interfaces

1. Introduction

While photovoltaic technology offers great potential as a renewable, alternative source of electrical energy, one of the main reasons that such potential is not yet fully utilized is the difficulty making such devices at a cost competitive with the cost of conventional energy sources. Therefore, the demand for inexpensive, renewable energy sources is a strong driving force for the research efforts on low-cost photovoltaic device technologies. In the last decades, much effort has been put into the development of solar cells based on organic molecules and conjugated polymers [1–9]. Polymeric materials have technological advantages over conventional inorganic materials in the reduction of production costs by large scale production, combined with the possibility to produce large area flexible devices and the tunability of the electronic bandgap by chemical synthesis. Until now, the best photovoltaic energy conversion efficiencies for different organic solid state solar cells are typically in the range of 1% [3,8,10].

For the generation of electrical power by illumination it is necessary to spatially separate the electron–hole (e–h) pair generated in the absorption process before geminate recombination takes place. In conjugated polymers, the separation of the photoexcited e–h pair can be achieved by blending the polymer with an acceptor molecule having an electron affinity which fulfills the inequality

$$I_p^* - E_a - U_{eff} < 0$$

where I_p^* is the ionization potential of the excited donor, E_a the electron affinity of the acceptor and U_{eff} all Coulomb correlations including the polarization effects. Under these conditions it is energetically favorable for the excited conjugated polymer to transfer an electron to the acceptor

* Corresponding author. Tel.: +43-732-2468-766; fax: +43-732-2468-770.
E-mail address: christoph.brabec@jk.uni-lin.ac.at (C.J. Brabec).

0379-6779/01/$ – see front matter
PII: S0379-6779(00)00276-9

molecule, while a hole remains in the polymer valence band. Conjugated polymers such as derivatives of poly(*para*-phenylenevinylenes) or polythiophenes exhibit an ultrafast photoinduced electron transfer to C_{60} with forward transfer faster than 100 fs in the solid state [11–13]. Thus, the quantum yield of the charge separation in such D/A blends is near unity. The charge separated state, however, is metastable at low temperatures. This photophysical process, resembling the primary steps of photosynthesis, has been utilized to fabricate solar cells [6–9]. Studies of conjugated polymer/fullerene photovoltaic devices showed that the energy conversion efficiency is limited by saturation of the photocurrent at high light intensities, which is assigned to loss mechanisms during the collection of the charges at the electrodes [8,14]. This is mainly due to the unbalanced transport of the charge carriers, a consequence of the different mobilities of the single compounds, i.e. holes on the conjugated polymer and electrons on the fullerenes, leading to different effective mean free paths.

The performance of such *bulk heterojunction* devices is significantly enhanced compared to devices made from single components and at least equivalent to optimized donor–acceptor bilayer devices [15]. For devices working with an interpenetrating network of donors and acceptors carrier collection efficiencies as high as 29% and monochromatic power conversion efficiencies between 3 [8] and 5% [9] have been reported. Additionally, large area plastic solar cells with comparable performance based on a composite from poly(2-methoxy-5-(3′,7′-dimethyloctyloxy)-1,4-phenylene vinylene) (MDMO-PPV) and (phenyl-[6,6]-C_{61})-butyric acid methyl ester (PCBM) have been recently demonstrated [16–18].

The rather high efficiencies of the bulk heterojunction photovoltaic devices have been achieved using phase-separated composite materials through control of the phase-separation into an interpenetrating network of organic donors and acceptors sandwiched between two electrodes with different work functions. Due to the necessity of bipolar charge transport in the bulk of such devices a strong connection between the efficiency and the morphology is expected.

Recently it has been shown that comparable efficiencies can be obtained for photovoltaic devices produced from alkoxy substituted PPVs with PCBM and also with C_{60} [8,14]. While the excellent film forming properties of MDMO-PPV with fullerene-based acceptors are well known, the class of substituted polythiophenes is known to show a higher tendency of phase separation with fullerenes [19]. Due to this, photovoltaic devices based on blends of polythiophenes with fullerenes have not been investigated as extensively as their PPV pendants. It is, therefore, interesting to compare these two different classes of conjugated polymers with respect to their photovoltaic behavior in composite films with fullerenes. The quality and homogeneity of the composite film brings several other implications concerning the efficiency of the solar cell. Inhomogeneous films with pinholes and/or a large serial resistivity lead to small fill factors (FF), lower rectification and decreased open circuit voltages (V_{oc}). In addition, it has been clearly shown that by decreasing the device thickness to an optimum value the efficiency can be increased significantly [20]. For the processing of pinhole free thin film devices excellent control over the film morphology is compulsory.

In this study, we present polymeric photovoltaic devices based on the following composites: MDMO-PPV/PCBM (1:3 weight ratio), poly(3-octylthiophene) (P3OT)/C_{60} (1:1 weight ratio), P3OT/PCBM monoadduct and multiadduct (1:2 weight ratio). While PCBM monoadduct has one side group, PCBM multiadduct has two or three of the same side groups attached to the sphere in a variety of relative positions.

All devices were produced on 6 cm×6 cm large semi-transparent ITO coated polyester foil with an active area of 16 cm^2. Using a polymer foil instead of glass substrates is important for the production of plastic solar cells on an industrial scale, because polymer foils are easier to handle in processing steps like cutting of large entities into smaller individual modules, laminating etc. Devices were characterized by current voltage (*I/V*) measurements under monochromatic light as well as by wavelength dependent photocurrent measurements. From these data power efficiencies were calculated and compared to carrier collection efficiencies (incident photon to converted electron, IPCE). For all devices, the surface morphology was investigated by atomic force microscopy (AFM).

2. Experimental

The device configuration and device preparation for polymeric photovoltaic cells (and photodetectors) were described before [8,12,21]. The photovoltaic devices consist of four layers as shown in Fig. 1. The photoactive materials used are: MDMO-PPV (supplied by COVION), P3OT (supplied by Neste Oy) and PCBM (synthezied by J.C.H.). First the PEDOT-PSS (poly(3,4-ethylenedioxythiophene)-poly(-styrenesulfonate) (Baytron–Bayer AG) was spin coated (thickness approximately 100 nm) on transparent ITO (indium tin oxide)-coated polyester substrates with typical areas of 6 cm×6 cm (surface resistance of 55 Ω/cm^2). Subsequently, the photoactive layer was produced by spin coating films of the composites: MDMO-PPV/PCBM (1:3 weight ratio), P3OT/C_{60} (1:1 weight ratio), P3OT/PCBM monoadduct and P3OT/PCBM multiadduct (both 1:2 weight ratio) from xylene solutions on top of the PEDOT-PSS layer. The enhanced solubility of PCBM [22] compared to C_{60} allows a high fullerene/conjugated polymer ratio in donor–acceptor bulk heterojunctions. After an additional drying step the aluminum top electrode was deposited by vacuum evaporation. The thickness of the polymer/fullerene layers as monitored by Dektak and optical absorption measure-

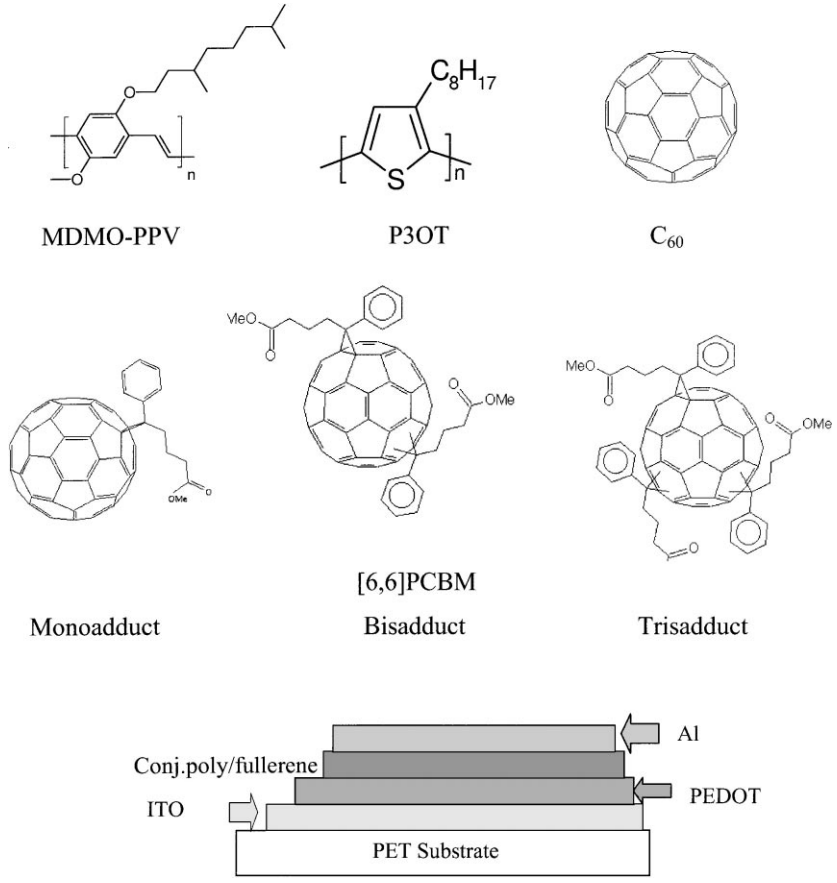

Fig. 1. Schematic diagram of the device configuration and molecular structures of the materials used.

ments was typically in the range of 120–150 nm. Exchanging the type of fullerene for the P3OT devices varied the film thickness by less than 10%.

All cells were produced under ambient conditions. No actions were taken to remove possibly adsorbed oxygen from the cells. A defocused Ar^+ laser beam at 488 nm provided illumination. Optical absorption was recorded with a Hitachi spectrophotometer. Light intensities were measured by a calibrated Si Photodiode. A Keithley SMU 2400 Source Meter was used to record the *I/V* curves by illuminating the cells through the ITO side, typically by averaging 80 measurements for one point.

3. Results and discussion

All solar cells were produced in the sandwich geometry as mentioned above, i.e. between two metal electrodes with different work functions, ITO (ϕ_{ITO}~4.7 eV) as anode (hole collector) and aluminum (ϕ_{Al}=4.3 eV) as cathode (electron collector). Although the work function of ITO is a poorly defined quantity (values ranging from 5.5 [23] to 4.1 eV [24] are reported in literature), recent estimates seem to converge into the range between 4.5–4.9 eV [25,26]. Asymmetric work functions of the electrodes in these interpenetrating network photovoltaic devices are important: It has been shown that in such devices charge separation, migration and collection at the corresponding electrodes are favorably tuned by an external electric field [27]. Without this built-in field there will be no selection principle for the holes to travel to the ITO and for the electrons to go to the aluminum electrode. At fullerene concentrations higher than the percolation threshold of 17 vol.% [18] this electric field separates the non-equilibrium carriers generated by the incident light and a short circuit current is delivered to the electrodes.

The calculation of the overall energy conversion efficiency, η_e has been performed using the equation

$$\eta_e = \frac{(V_{oc}(\mathrm{V}) \times I_{sc}(\mathrm{A/cm^2}) \times \mathrm{FF})}{P_{inc}(\mathrm{W/cm^2})}$$

under different intensities, where V_{oc}, I_{sc}, FF and P_{inc} are the open circuit potential, short circuit current, filling factor and incident light power, respectively. We determine the value of the fill factor of the device, FF, by calculating the area of the maximum power rectangular area under the *I/V* curve in the fourth quadrant. Therefore, the filling factor is given by

$$\mathrm{FF} = \frac{(V_{max} \times I_{max})}{(V_{oc} \times I_{sc})},$$

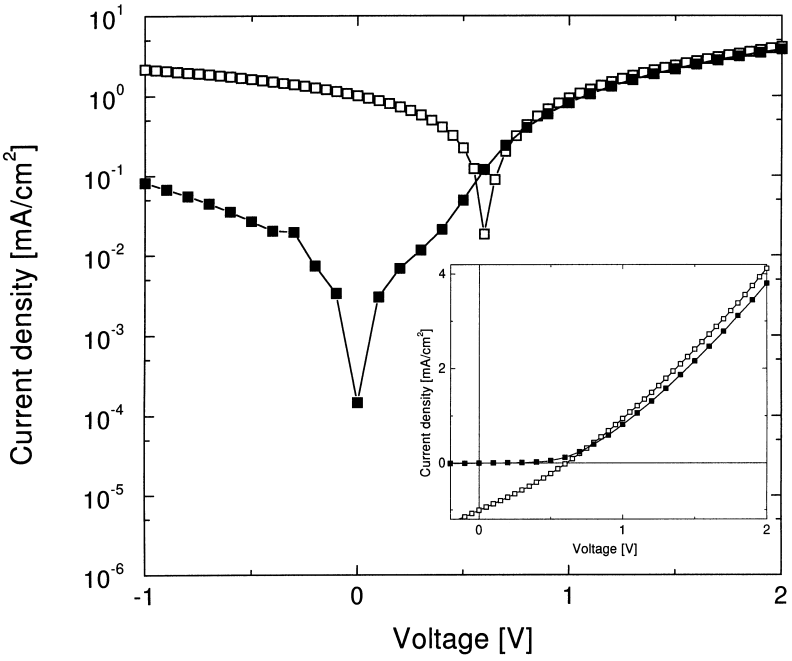

Fig. 2. *I/V* characteristics of ITO/PEDOT/MDMO-PPV:PCBM /Al (solid squares: dark, open squares: illuminated with 488 nm, 20 mW/cm^2) flexible large area plastic solar cell in a logarithmic scale. The inset is a linear plot of the *I/V* data for positive voltage.

where V_{max} and I_{max} are voltage and current, respectively, at the point of maximum power output.

For this comparative study a photovoltaic device produced from MDMO-PPV/PCBM is presented and discussed first. Fig. 2 shows the *I/V* characteristics of an ITO/PEDOT/MDMO-PPV:PCBM/Al flexible large area plastic solar cell on a linear as well as logarithmic scale. Because of the logarithmic scale of the current axis, the absolute value of the current is plotted against the voltage. The characteristic values of the device in Fig. 2 are $V_{oc}\sim$600 mV, $I_{sc}\approx$1 mA/cm^2 and a fill factor FF$\sim$0.3 under monochromatic illumination (488 nm) with 20 mW/cm^2. Open circuit voltages higher than 800 mV were observed for these devices. The rectification of this device is $\sim$10 at $\pm$1 V in the dark while under illumination the forward and reverse current are found to be almost symmetrical at $\pm$2 V. At higher forward bias, the dark and the photocurrent are comparable to each other, indicating that photoconductivity does not play an important role for this device. The dark *I/V* curve shows a small change in the curvature at 0.5 V. Between -0.5 and $+0.5$ V the logarithmically plotted dark current is rather symmetric to the 0 V center for positive and negative applied voltages. Such a symmetry can be explained by the contribution of a small shunt resistivity to the diode current. Small shunts manifest as 'Ohmic' behavior in the low current regime of a diode. For identically produced devices with smaller active areas (<1 cm^2) a FF as high as 0.45 was observed. The decrease of the FF with increasing device area indicates the loss of film quality due to the upscaling.

In Fig. 3 the characteristics of an ITO/PEDOT/P3OT:C_{60}/Al flexible large area plastic solar cell are plotted in a linear and logarithmic scale. The characteristic data of this cell are an open circuit voltage of $\sim$600 mV, a short circuit current of approximately 1.06 mA/cm^2 and a FF of 0.3. The rectification of this device in the dark at $\pm$1 V ($\sim$6) is lower than for the MDMO-PPV/PCBM device presented in Fig. 2. A change in the curvature of the dark *I/V* curve at $\sim$0.5 V is observed together with a highly symmetric current/voltage behavior around 0 V in the logarithmic plot between $\pm$0.5 V. In the forward direction at higher voltages, dark current and photocurrent show comparable values and no dominant photoconductivity is observed.

The current/voltage characteristics for a device with P3OT and PCBM monoadduct as the photoactive layer are presented in Fig. 4. The *I/V* data of the ITO/PEDOT/P3OT:PCBM/Al flexible large area plastic solar cell are plotted again in a linear and logarithmic scale. The typical data of this device under monochromatic illumination (488 nm) with 20 mW/cm^2 are: $V_{oc}\sim$600 mV, and FF=0.27. Even though the enhanced solubility of PCBM compared to C_{60} allows the preparation of higher fullerene concentrated solutions, using PCBM monoadduct we obtain a significant smaller short circuit current of $\sim$0.63 mA/cm^2 compared to the short circuit current for the P3OT:C_{60} device (1.06 mA/cm^2). The rectification of the P3OT:PCBM monoadduct devices ($\sim$15 at $\pm$2 V, $\sim$13 at $\pm$1 V) in the dark is comparable with the other devices. However, the P3OT:PCBM monoadduct device distinguishes significantly from the other devices by its *I/V* behavior in forward direction. While the MDMO-PPV:PCBM and the P3OT:C_{60} devices did not exhibit photoconductivity, the P3OT:PCBM monoadduct diode shows significant photo-

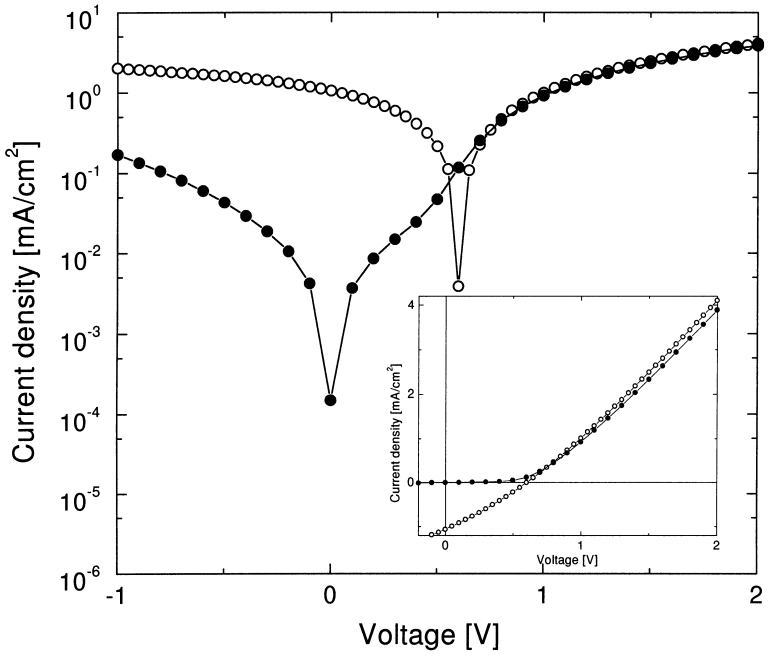

Fig. 3. Characteristics of the ITO/PEDOT/ P3OT:C_{60}/Al (solid circles: dark, open circles: illuminated with 488 nm, 20 mW/cm^2) flexible large area plastic solar cell in a logarithmic scale. The inset is a linear plot of the *I/V* data for positive voltage.

conductivity effects. At +2 V a photocurrent of ~3 mA/cm^2 is observed, while the dark current is measured with ~2 mA/cm^2. For the other two devices, both, the dark and the photocurrent were ~4 mA/cm^2. The observed photoconductivity indicates that in these composites bipolar charge transport is restricted. Additionally, the serial resistivity of this device is significantly higher than for the other material combinations as seen by the overall lower current in forward direction. A derivative-like feature is observed in the *I/V* curve at around +0.5 V when the P3OT/PCBM device is measured in the dark. The origin of this derivative like feature is not clear. Similar anomalies were observed in

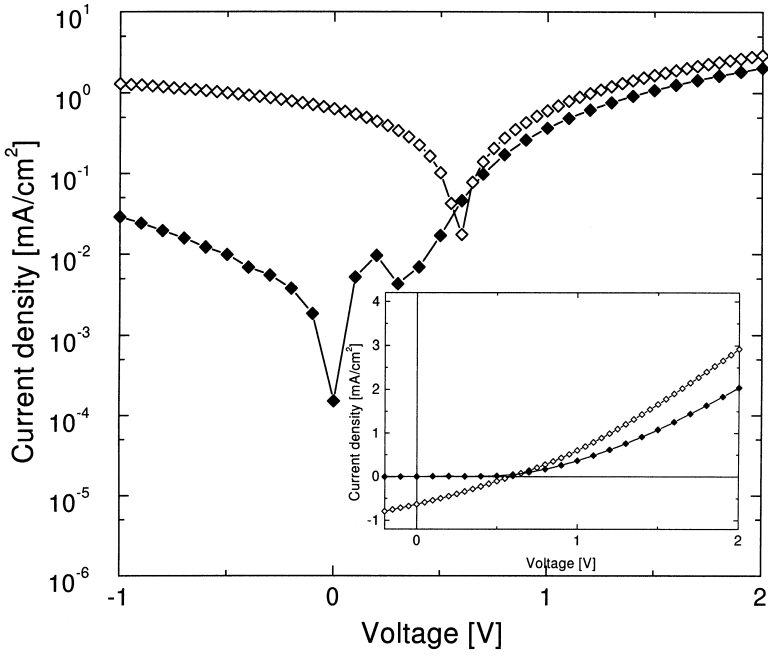

Fig. 4. ITO/PEDOT/P3OT:PCBM monoadduct/Al (solid diamonds: dark, open diamonds: illuminated with 488 nm, 20 mW/cm^2) flexible large area plastic solar cell in a logarithmic scale. The inset is a linear plot of the *I/V* data for positive voltage.

Table 1
I_{sc}, V_{oc}, I_{photo} (+2 V) and I_{dark} (+2 V) for P3OT/fullerene acceptor devices[a]

	I_{sc} (%)	V_{oc} (%)	I_{photo} (+2 V) (%)	I_{dark} (+2 V) (%)
P3OT:C60	100	100	100	96
P3OT:PCBM monoadduct	61	100	70	50
P3OT:PCBM multiadduct	28	100	43	27

[a] The I_{sc} and V_{oc} values are normalized to the data of the P3OT:C_{60} device, while the I_{photo} (+2 V) and I_{dark} (+2 V) are normalized to the I_{photo} (+2 V) of the P3OT:C_{60} device.

the *I/V* characteristics of organic multi-layer light emitting diodes [28].

PCBM multiadduct is rather similar to PCBM monoadduct from its electronic properties while the solubility, the film forming properties and the tendency against crystallization are enhanced compared to the monosubstituted methanofullerene. The multiadduct is, therefore, an excellent candidate to prove whether the results observed for P3OT:C_{60} and P3OT:PCBM monoadduct follow a trend or not. The relevant data of the *I/V* characteristics of a ITO/PEDOT/P3OT:PCBM multiadduct/Al flexible large area plastic solar cell are compared to the results of the other P3OT devices in Table 1. The values in Table 1 (I_{sc}, I_{photo}(+2 V), I_{dark} (+2 V), V_{oc}) are normalized to the results for the P3OT:C_{60} device. From Table 1 it is seen that the multiadduct device has enhanced photoconductivity and increased serial resistivity and confirms the tendency observed for the PCBM monoadduct and pristine C_{60} containing devices.

Also seen from Table 1 the P3OT:C60 system gives the best photovoltaic response of all the P3OT devices investigated in this study. Fig. 5 compares the *I/V* characteristics of the MDMO-PPV:PCBM reference photovoltaic device with the P3OT:C_{60} device under illumination and in the dark. We obtained comparably high I_{sc} values for the devices made from P3OT and MDMO-PPV blended with C_{60} and PCBM, respectively. The typical V_{oc} values for our large area devices on flexible ITO covered polyester substrates are around 600 mV. Even higher open circuit voltages (up to 800 mV) were observed for small area (<1 cm^2) spin cast devices on high quality ITO glass. The difference between the small and large area diodes is explained by a slight increase of the number of shunts for the large area devices. The value of the open circuit voltage for the bulk heterojunction devices is frequently interpreted (within the metal-insulator-metal MIM tunneldiode picture) as a function of the work function difference of the two electrodes (Al=4.3 eV; ITO=4.7 eV) which would yield a V_{oc} of

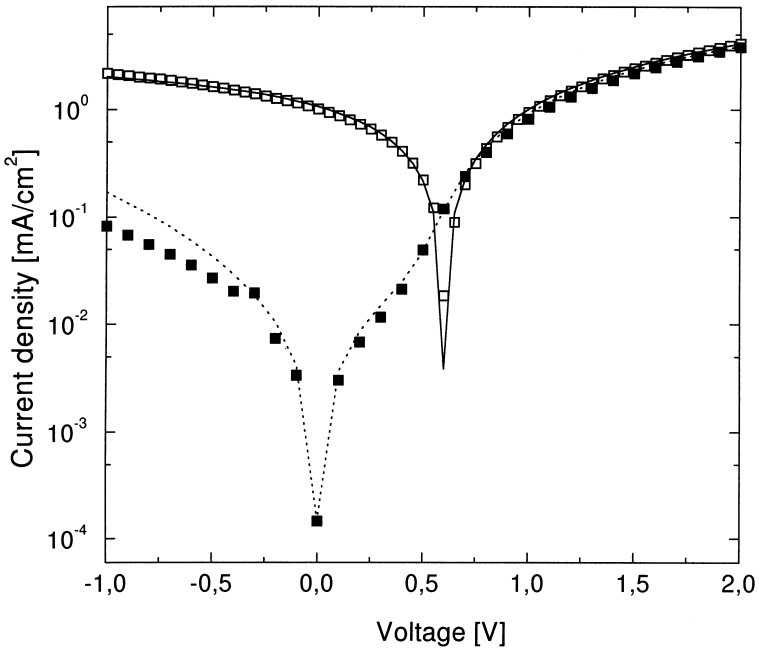

Fig. 5. *I/V* characteristics comparison of ITO/PEDOT/MDMO-PPV:PCBM/Al (open squares) and ITO/PEDOT/P3OT:C_{60}/Al (solid line) under illumination with 20 mW/cm^2 of an argon laser (488 nm). The solid squares and the dotted line show the *I/V* curves of the ITO/PEDOT/MDMO-PPV:PCBM/Al and ITO/PEDOT/ P3OT:C_{60}/Al devices, respectively, in the dark.

400; or lower, as was found by other groups [29,30]. The experimentally observed V_{oc} is clearly not consistent with this picture. The contribution of the PEDOT layer to this observed V_{oc} is not clear. The formation of space charge layers at the electrode/polymer interface may lead to local potentials influencing the open circuit potential. Capacitance measurements were performed and the dependence of the built-in field on the work function of the electrodes was investigated to characterize the nature of the inorganic/organic interfaces in interpenetrating network solar cells. The formation of localized dipole layers at the electron collecting metal/organic semiconductor interface (cathode) was observed in conjugated polymer/fullerene photovoltaic devices [31].

The overall energy conversion efficiency, η_e, for the P3OT/C_{60} as well as for the MDMO-PPV/PCBM flexible plastic solar cells was calculated to be approximately 1.5% under monochromatic 10 mW/cm^2 illumination (488 nm) [16,17,20,32].

The photovoltaic external quantum efficiency (charge carrier per incident photon) or the spectrally resolved incident photon to converted electron efficiency IPCE (η_c) is calculated from the spectrally resolved short-circuit current,

$$\eta_c(\%) = \frac{1240}{\lambda(\mathrm{nm})} \times \frac{I_{sc}(\mu\mathrm{A/cm^2})}{I_{inc}(\mathrm{W/m^2})},$$

where I_{inc} is the intensity of the incident light. The maximum value of the electron to photon conversion efficiency of an MDMO-PPV/PCBM solar cell is found to be about 20% at 488 nm, which is comparable to earlier reports [16]. On the other hand for a P3OT/C_{60} flexible large area plastic solar cell we also achieved an IPCE of ~20% (I_{sc} of ~800 μA/cm^2 under an argon laser at 488 nm with 10 mW/cm^2) [32].

Fig. 6 shows the dependence of the short circuit current on the incident light intensity, which follows a power law $I_{sc} \sim I^{\alpha}$. The scaling exponent α was fitted to 0.89 and 0.93 for ITO/PEDOT/MDMO-PPV:PCBM/Al (solid circles) and ITO/PEDOT/P3OT:C_{60}/Al (open circles) photovoltaic devices, respectively, between 0.01 and 10 mW/cm^2. At higher intensities I_{sc} is limited either by bimolecular recombination or saturation behavior. For the large area photovoltaic devices investigated in this study both processes may be relevant. Scaling exponents close to 1 are expected for devices, where both electron and hole transport are comparably efficient and bimolecular recombination not significant. Low charge carrier mobilities in the pristine components (PPV~10^{-4} cm^2/V s [33–35] and C_{60}~10^{-2} cm^2/V s [36] are expected to give an upper limit for the photocurrent. However, due to the phase separation or aggregation of the two components inside the interpenetrating network, the overall mobility of the network might be lower than the mobilities of the single components.

The *I/V* studies for P3OT photovoltaic devices with different acceptors discussed above already gave indications that the photovoltaic conversion efficiency is strongly related to the interpenetrating network morphology for bipolar devices. Therefore, we investigated the surface morphology of the composite materials using atomic force microscope (AFM). Fig. 7 illustrates an AFM comparison of MDMO-PPV/PCBM (a), P3OT/C_{60} (b), P3OT/PCBM monoadduct (c) and P3OT/PCBM multiadduct (d) composite films. The pictures were taken directly from the devices after the *I/V* measurements. MDMO-PPV/PCBM composite films show rather homogeneous films without pinholes. P3OT/C_{60} composite films show very homogeneous films in the sub-μm scale. In contrast, the P3OT/PCBM monoadduct films show strong phase separation on a horizontal scale of several μm. Pinholes with depths of ~30 nm are observed in the P3OT/PCBM films. The AFM results confirm the findings from *I/V* spectroscopy. Substituting C_{60} by PCBM monoadduct in a P3OT matrix introduces enhanced phase separation in the interpenetrating network, thus leading to lower short circuit currents, more pronounced photoconductivity and higher serial resistivities. The AFM picture of the P3OT:PCBM multiadduct is more complicated to interpret. The surface of this composite is rather unstructured and homogenous. Several crater like features with sub-μm size are observed. Within the center of these craters, pinholes with depths of >50 nm and a width of ~100 nm diameter are located. Such features are not observed in the pristine polymer films and must be related to the presence of PCBM multiadduct in the composite. Molecule specific studies are necessary to determine whether the surface consists of the pristine acceptor PCBM multiadduct or of a blend of P3OT with PCBM multiadduct.

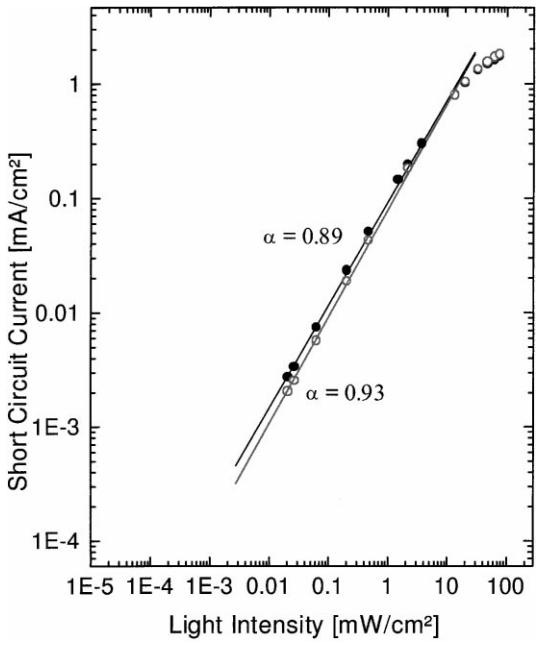

Fig. 6. Dependence of the short circuit current versus incident light intensity of an ITO/PEDOT/P3OT:C_{60}/Al (open circles) and ITO/PEDOT/MDMO-PPV:PCBM/Al (solid circles) flexible large area plastic solar cells. Lines are fits to a power law and are discussed in the text.

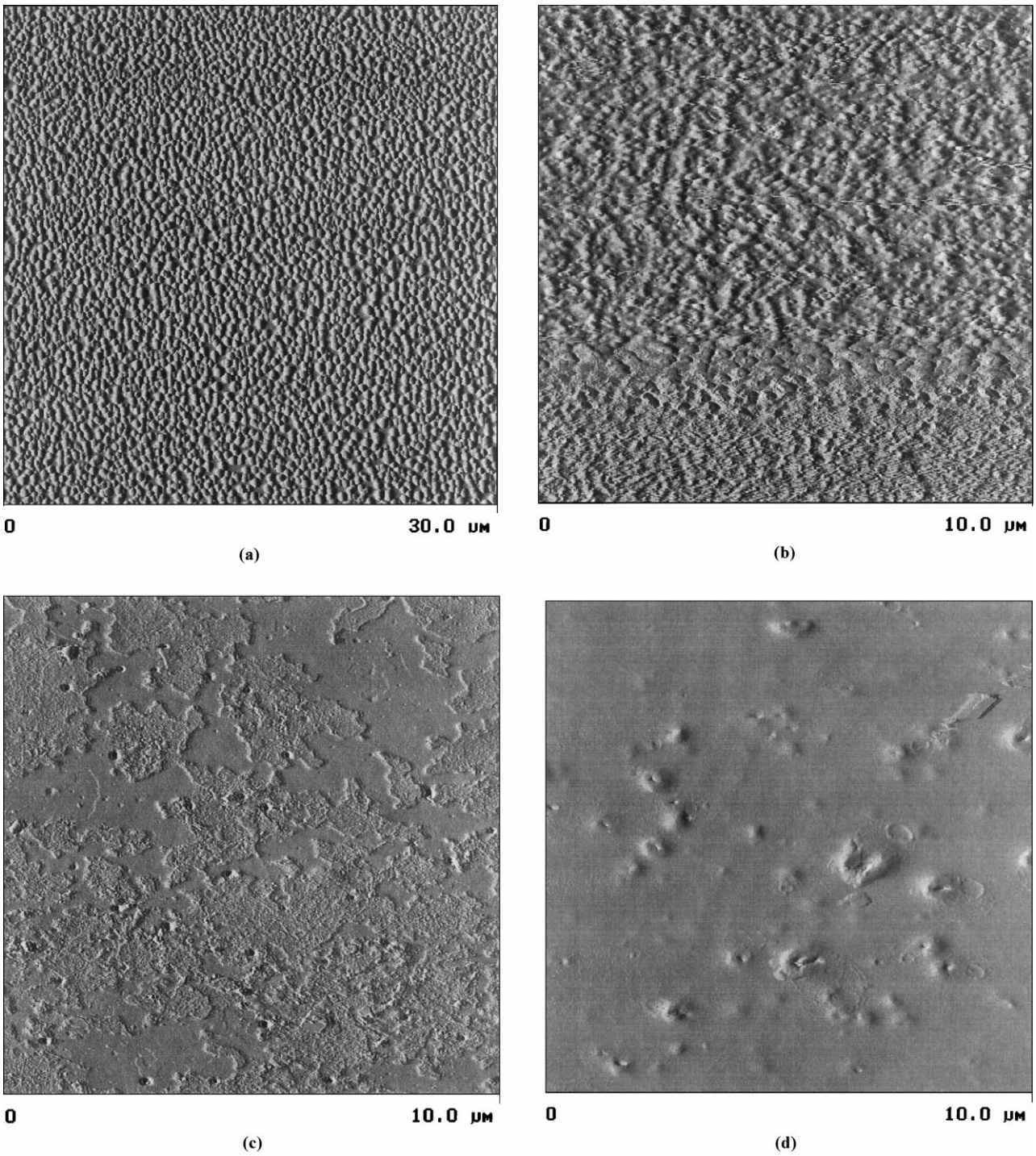

Fig. 7. AFM comparison of (a) MDMO-PPV/PCBM (1:3 weight ratio), (b) P3OT/C_{60} (1:1 weight ratio), (c) P3OT/PCBM monoadduct (1:2 weight ratio) and (d) P3OT/PCBM multiadduct (1:2 weight ratio) composite films.

4. Conclusion

Large area photovoltaic devices fabricated from several blends of MDMO-PPV and P3OT as donors and fullerene (C_{60}) and methanofullerene (PCBM) as acceptors show open circuit voltages up to 600 mV and short circuit currents up to 1 mA/cm^2 under monochromatic illumination (488 nm) with 20 mW/cm^2. Large area flexible plastic solar cells can be fabricated with P3OT:C_{60} blends. These cells are equally efficient as the MDMO-PPV/PCBM large area flexible plastic solar cell. Under 10 mW/cm^2 monochromatic light at 488 nm the overall energy conversion efficiency, η_e, of a P3OT/C_{60} flexible plastic solar cell presented here is calculated to be around 1.5% with a FF=0.3 and an

IPCE of nearly 20%. Detailed analysis of *I/V* curves combined with AFM spectroscopy allowed a precise evaluation of the performance of photovoltaic devices based on P3OT and different fullerene acceptors. P3OT:C_{60} formed pinhole free and homogenous films on the sub-μm scale. In films of P3OT with more soluble methanofullerenes (PCBM monoadduct and multiadduct) phase separation and pinholes were observed. Consequently, these devices exhibited lower conversion efficiency, enhanced photoconductivity and higher serial resistivities.

Acknowledgements

This work was performed within the Christian Doppler Foundation's dedicated Laboratory for Plastic Solar Cells funded by the Austrian Ministry of Economic Affairs and Quantum Solar Energy Linz Ges.m.b.H. Financial support from Austrian Foundation for Advancement of Science (FWF P12680 CHE), from the European Commission JOULE III Programme (JOR3-CT98-0206), the Magistrat Linz and The Netherlands Organization for Energy & Environment (NOVEM) are gratefully acknowledged. D. Gebeyehu is financed by the Austrian Academic Exchange Office (ÖAD) graduate scholarship program.

References

[1] J. Simon, J.-J. Andre, Molecular Semiconductors, Spring, Berlin, 1985.
[2] M. Kaneko, in: H.S. Nalwa (Ed.), Handbook of Organic Conductive Molecules and Polymers, Vol. 4, Wiley, New York, 1997, p. 661.
[3] C.W. Tang, Appl. Phys. Lett. 48 (1986) 183.
[4] D. Wöhrle, D. Meissner, Adv. Mat. 3 (1991) 129.
[5] S. Günster, S. Siebentritt, J. Elbe, Kreienhoop, B. Tennigkeit, D. Wöhrle, R. Memming, D. Meissner, Mol. Crystal Liq. Crystal 218 (1992) 117.
[6] N.S. Braun, D. Sariciftci, C. Zhang, V. Srdanov, A.J. Heeger, G. Stucky, F. Wudl, Appl. Phys. Lett. 62 (1992) 585.
[7] S. Moria, A.A. Zakhaidov, K. Yoshino, Sol. State Commun. 82 (1992) 249.
[8] G.Yu.J. Gao, J.C. Hummelen, F. Wundl, A.J. Heeger, Science 270 (1995) 1789.
[9] M. Granström, K. Petritsch, A.C. Arias, A. Lux, M.R. Andersson, R.H. Friend, J. Nature 395 (1998) 257.
[10] J. Rostalski, D. Meissner, Proceedings of European Conference on Organic Solar Cells, ECOS 98 Cadarache, France, Solar Energy Materials and Solar Cells, in press.
[11] N.S. Sariciftci, L. Smilowitz, A.J. Heeger, F. Wudl, Science 258 (1992) 1474.
[12] N.S. Sariciftci, A.J. Heeger, in: H.S. Nalwa (Ed.), Handbook of Organic Conductive Molecules and Polymers, Vol. 1, Wiley, New York, 1997, p. 437.
[13] C.J. Brabec, G. Zerza, N.S. Sariciftci, G. Cerullo, S. De-Silvestri, S. Luzatti, J.C. Hummelen, submitted for publication.
[14] J. Gao, H. Wang, F. Hide, Synth. Met. 84 (1997) 979.
[15] C.J. Brabec, N.S. Sariciftci, in: G. Hadjioannou, P. van Hutten (Eds.), Semiconducting Polymers, Wiley-VCH, Weinheim, 1999, pp. 515.
[16] C.J. Brabec, F. Padinger, J.C. Hummelen, R.A.J. Janssen, N.S. Sariciftci, Synth. Met. 102 (1999) 861.
[17] C.J. Brabec, F. Padinger, N.S. Sariciftci, J. Appl. Phys. 85 (1999) 6866.
[18] C.J. Brabec, F. Padinger, V. Dyaknov, J.C. Hummelen, R.A.J. Janssen, N.S. Sariciftci, in: Kuzmany, Fink, Mehring, Roth (Eds.), Electronic Properties of Novel Materials — Progress in Molecular Nanostructures, World Scientific Publishing, 1998, p. 519.
[19] N.S. Sariciftci, in: H.S. Nalwa (Ed.), Handbook of Organic Conductive Molecules and Polymers, Vol. 1, Wiley, New York, 1997, p. 414.
[20] T. Fromherz, F. Padinger, D. Gebeyehu, C. Brabec, J.C. Hummelen, N.S. Sariciftci, Proceedings of European Conference on Organic Solar Cells, ECOS 98, Cadarache, France, Solar Energy Materials and Solar Cells, in press.
[21] N.S. Sariciftci, J. Prog. Quant. Electr. 19 (1995) 131.
[22] J.C. Hummelen, B.W. Wright, F. Wudl, F. Lepec, J. Org. Chem. 60 (1995) 532.
[23] T. Ishida, H. Kobayashi, Y. Nakato, J. Appl. Phys. 73 (1993) 4344.
[24] J. Shewchun, J. Dubow, C.W. Wilmsen, R. Singh, D. Burk, J.F. Wager, J. Appl. Phys. 50 (1979) 2832.
[25] Y. Park, V. Choong, Y. Gao, B.R. Hsieh, C.W. Tang, Appl. Phys. Lett. 68 (1996) 2699.
[26] I.D. Parker, J. Appl. Phys. 75 (1994) 1656–1666.
[27] Y. Wang, A. Suna, J. Phys. Chem. B 101 (1997) 5627.
[28] S. Berleb, W. Brüttinger, M. Schwörer, Proceedings of Inernational Conference on Synthetic Metals, ICSM 1998, Montpellier, France, Synth. Met., in press.
[29] L.R. Roman, M.R. Anderson, T. Yohannes, O. Inganäs, Adv. Mater. 9 (15) (1997) 1164.
[30] K. Yoshino, K. Tada, M. Hirohata, H. Kajii, Y. Hironaka, N. Tada, Y. Kaneuchi, M. Yoshida, A. Fijii, M. Hamagchi, H. Araki, T. Kawai, M. Ozaki, Y. Ohmri, M. Onoda, A.A. Zakhidov, Synth. Met. 84 (1997) 477.
[31] C.J. Brabec, T. Fromherz, J.C. Hummelen, N.S. Sariciftci, in preparation.
[32] F. Padinger, T. Fromherz, C. Brabec, D. Gebeyehu, J.C. Hummelen, N.S. Sariciftci, Proceedings of the 11th Workshop on Quantum Solar Energy Conversion, QUANTSOL 99, Wildhaus, Switzerland.
[33] C.H. Lee, G. Yu, A.J. Heeger, Phys. Rev. B 47 (1993) 15543.
[34] S. Karg, M. Meier, W. Riess, J. Appl. Phys. 82 (1997) 1951.
[35] G.H. Gelink, J.M. Warman, J. Phys. Chem. B 100 (1996) 20035.
[36] C.H. Lee, G. Yu, D. Moses, V.I. Srdanov, X. Wei, Z.V. Vardeny, Phys. Rev. B 48 (1993) 8506.